Orbit Propagation and Validation with Angle-Only Observations

Carolin Früh* and Thomas Schildknecht†
University of Bern, Bern, 3012, Switzerland

Abstract

With the growing number of resident space objects (RSOs) precise orbit determination and prediction plays an increasingly important role. In the scope of protecting operational spacecraft very accurate orbit prediction is a prerequisite. Predicting close conjunctions and assessing collision probabilities well in advance on a reliable confidence level enables planning and performing of collision avoidance manoeuvres. With sophisticated post-processing methods, when all information is available accuracies in the order of centimeters can be achieved. Post-processing of surveillance data (optical, radar) is still assumed to be in the order of meters. The accuracy of orbit prediction rather than a post-fit of data of common operational products is inferior by orders of magnitudes.

This paper addresses the task of orbit propagation based on angle-only observations of RSOs in geostationary and high eccentricity orbits. The focus is on objects which do not perform manoeuvres, to clearly separate the effects of manoeuvre data – which is probably unavailable and/or inaccurate – from modeling the natural forces. The angle-only observations stem from the one-meter ZIMmerwald Laser and Astrometry Telescope (ZIMLAT), the 18-cm Zimmerwald SMall Robotic Telescope (ZimSMART), both located in Zimmerwald, close to Bern, Switzerland, and from the one-meter ESA Space Debris Telescope (ESASDT) located on Tenerife, Spain. The one-meter telescopes have been used for RSO surveys and for so-called follow-up observations over the past decade by the Astronomical Institute of the University of Bern, which is a prime contractor of the European Space Agency (ESA) in the fields of Surveillance and Tracking. Supplementary observations are provided by the courtesy of the International Scientific Optical Network (ISON).

Orbit determination and propagation is performed with an enhanced version of the CelMech tool (Beutler, *Methods of Celestial Mechanics*, Springer 2001). The force model used includes Earth's potential coefficients up to order and degree 12, perturbations due to earth tides, and corrections due to general relativity. Earth shadow passages are modeled. In addition, a model for estimating the direct radiation pressure (DRP) is used, which allows an estimate of the area to mass ratio as a scaling factor, as well as the osculating elements. Optionally, biases, which account inter alia for asymmetries in the observed object, e.g. misalignment of solar panels, can be estimated. Orbit propagation is performed using the determined osculating elements, the estimated area to mass ratio, and the reflection coefficient within the force model mentioned above. The estimated biases are not available for orbit propagation. The ephemerides of the propagated orbits are compared to observations of the same object, which were not used for orbit determination. Those additional angle-only observations serve as ground truth. The additional observations that belong to the same object are validated by a further orbit determination including all observations. The influence of the temporal spacing of observations and the effect of fusing data of different observation sites is investigated. As a reference, two line element data (TLEs) of the US Strategic Command (USSTRATCOM) catalogue are propagated with the SDP4 propagator and the resulting ephemerides are compared to the angle-only observations. Covariances for the TLE data are then estimated.

* Research Astrodynamicist, Astronomical Institute, University of Bern, Sidlerstrasse 5, 3012 Bern, Switzerland, +41 31 631 8819, frueh@aiub.unibe.ch

† Professor, Astronomical Institute, University of Bern, Sidlerstrasse 5, 3012 Bern, Switzerland, +41 31 631 8594, thomas.schildknecht@aiub.unibe.ch

1 Introduction

The Astronomical Institute of the University of Bern (AIUB) has performed optical surveys of the geostationary orbits (GEO) and geostationary transfer (GTO) and other highly eccentric orbits (HEO) for over ten years. For this process, AIUB tasks the one-meter telescope ZIMmerwald Laser and Astrometry Telescope (ZIMLAT) and recently the Zimmerwald SMall Robotic Telescope (ZimSMART), both in Zimmerwald close to Bern, Switzerland, and the ESA Space Debris Telescope (ESASDT) on Tenerife, Spain. Single angle-only observations are connected to tracklets. In the first step, circular orbits are determined. In the second step, follow-up observations are performed, which allow determination of a full six-parameter orbit. AIUB maintains an independent catalogue of space debris objects which overlaps only partly with the USSTRATCOM catalogue. To maintain this catalogue, to secure orbits, and to provide highly accurate predictions of these orbits, further observations over longer time periods are necessary. An initial determination of the spacing of the follow-up observations directly after discovery have been performed by Musci et.al.[1]. The accuracy of orbit determination from densely spaced observational data has been investigated in [2]. If a larger amount of objects is tracked in routine catalogue maintenance, optical angle-only observations on the other hand are normally not very dense. Due to bad weather or other circumstances, larger gaps within the data have to be faced. Orbit determination is performed with an accuracy level of the order of a few arcseconds for normal routine optical observations. Residuals for propagated orbits are remarkably higher. This paper investigates the orbit propagation of USSTRATCOM TLEs with different propagators and orbit determination and accuracy of propagation of sparse angle-only observations, which are gained in routine catalogue maintenance measurements. The aspect of spacing and merging observations of different observation sites are investigated.

2 Method of Investigation

Two different types of orbits are investigated in this paper: Orbits in the two line element format (TLE) – obtained from the USSTRATCOM catalogue – and internal orbits of the AIUB catalogue. In the case of the internal AIUB catalogue, orbits are determined from optical angle-only observations obtained from ZIMLAT, ZimSMART, and ESASDT, supplemented by some observations of the ISON network provided by the Keldish Institute of Applied Mathematics, Moscow, Russia. The latter observations were obtained from different sites of the ISON network, in this particular case, all located in Eastern Europe. The internal orbits are determined with a modified version of the so called CelMech tool, whose original version can be found in [3]. The force model used for orbit determination takes into account earth's potential coefficients of order and degree 12, perturbation of ocean and earth tides. Earth shadow passes are modeled and corrections due to general relativity are taken into account. The direct radiation pressure (DRP) is available as a solve-for parameter, which allows an estimate of the instantaneous effective area to mass ratio of objects. In addition, biases, which account inter alia for asymmetries in the observed object, e.g., misalignment of solar panels, can be estimated. The latter were only estimated if it was otherwise not possible to determine a good orbit. The CelMech tool allows setting further parameters as including once per revolution stochastic pulses. It turned out that those optimize the fit of the orbit to the observed data but turned out badly in propagation.

In the case of the TLEs, propagation is performed with the official SDP4 and SDP8 propagators [4]. In case of the internal orbits, propagation is performed with the CelMech tool again. Whereas the coefficient of the area to mass ratio, i.e., the estimation of the direct radiation pressure, can be used for propagation, estimated biases are not available for propagation. In both cases, the accuracy of the orbit propagation is determined with the COROBS tool, whose functionalities are described below. For further details, refer to Früh et al. [5]. The predicted ephemeris positions are compared to the optical angle-only observations, which were not used in orbit determination. Residuals are determined directly on the celestial sphere and in a projected intrack and crosstrack direction within the observational plane. This projection is preferred over taking into account the range and working with a three dimensional residual vector, since range information can only be gained via orbit determination, which introduces further constraints. The residuals in the projected intrack direction can have positive and negative values (that is in direction of the projected moving direction of the object (positive) and vice versa) whereas the projected crosstrack direction residuals and residuals on the celestial sphere can take only positive values, as defined in Früh et al. [5]. The observation used for the comparison stem from ZIMLAT, ZimSMART and ESASDT and serve as ground truth. At both sites regular comparisons of the observational data to independent sources are performed, e.g., comparison to GPS state vector data. The additional data which are used as a reference here are all cross-checked. Cross-checked means that further successful orbit determinations were performed with all data used as ground truth to ensure that they in fact belong to the very same object.

3 Propagation of TLEs

Orbital data is distributed courtesy of the US Strategic Command in the two line element (TLE) format and does not contain covariance information. Covariances estimated on the basis of a larger amount of optical data can be found in Früh et al. [5]. The covariances estimated there are based on propagation with SDP8 propagator and the best fitting TLEs to the observational epoch. Residuals that were determined are of the order of three degrees on the celestial sphere, 20 to 30 km in intrack and roughly 10 km in crosstrack

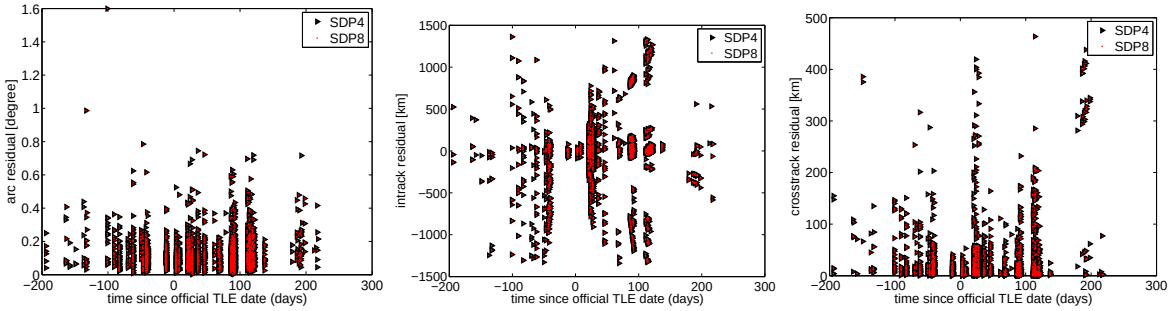

(a) *(b)* *(c)*

Figure 1: residuals in arc length on the celestial sphere(a), projected intrack (b) and crosstrack direction (c) with the SDP4 and SDP8 propagator for GEO objects

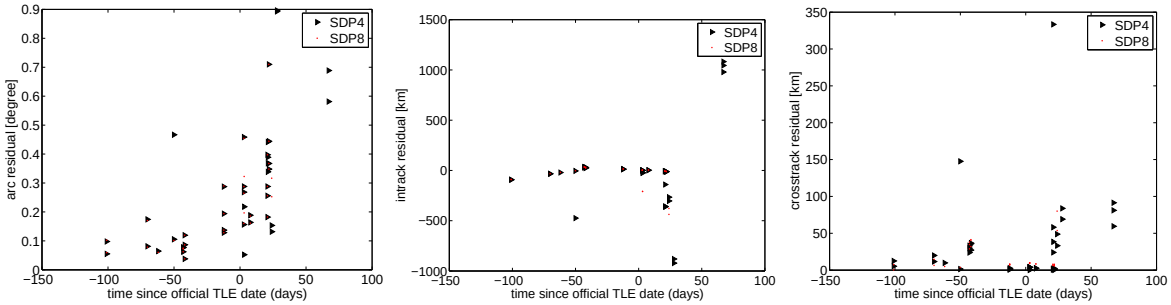

(a) *(b)* *(c)*

Figure 2: residuals in arc length on the celestial sphere(a), projected intrack (b) and crosstrack direction (c) with the SDP4 and SDP4 propagator for HEO objects

direction for objects in geostationary orbits and slightly higher of the order of five degrees, 35 and 25 km for objects in geostationary transfer and other highly eccentric orbits. On the other hand, it could be shown in Früh et al. [6] that the primary problem with the TLE data is the large fluctuations in single TLE data sets. To investigate that aspect further, single TLE data sets of 14 GEO objects and 8 HEO objects have been studied in further detail. One TLE set per object was propagated backward and forward in time and compared to optical observations with COROBS. The COSPAR numbers and epochs of the TLE sets used can be found in the appendix. The optical observations for the comparison stem from ZIMLAT and ZimSMART and were cross-checked by several orbit determinations with CelMech. The single epochs of the TLE data set were chosen under the premise to be covered best by the optical reference data. They differ from object to object. A similar analysis was performed in Kelso [7] with GPS precision ephemeris for the medium earth orbital (MEO) regime. There the SDP4 propagator was used and only the residuals in range were taken into account. Residuals in range are not displayed here, as explained in the previous section.

The comparison was performed twice for each object and data set independently with the SDP4 and the SDP8 propagator. The residuals for the GEO objects are displayed in Fig. 1: Fig. 1a shows the position residuals in degrees on the celestial sphere, Fig. 1b the projected intrack, and Fig. 1c the projected crosstrack residuals as a function if time relative to the official TLE epoch. First, it should be noted that the differences in the residuals obtained from the propagation of SDP4 and SDP8 are negligible in the GEO orbital regime. The classical expected “butterfly” shape (as it was also found in Kelso [7] with the GPS data in MEO) in the data around the official TLE epoch can only be seen in the intrack residuals. It was expected to see “half-butterfly” due to the positivity of the data in the arc and crosstrack residuals, which is not the case. There are cases where the intrack residuals are small and the crosstrack residuals are large. The observations are cross-checked and orbit determination showed that they in fact belong to the regarded objects; the large crosstrack residuals do not result from one single object. Intrack and crosstrack residuals, when viewed together reveal that there is not a prominent decrease in residuals around the official epoch of the TLEs. Even around that epoch, residuals are still of the order of over 0.2 degrees. There is also no remarkable decrease of residuals at other epoch, either.

The results for the HEO objects are displayed in Fig. 2. Fig. 2a shows the position residuals in degrees on the celestial sphere, Fig. 2b the projected intrack, and Fig. 2c the projected crosstrack residuals as a function of time relative to the official TLE epoch. Due to standard surveys and follow-up schemes performed at the Zimmerwald observatory, significantly less data is available. What can be

seen nevertheless is, that SDP4 produces smaller residuals, although the differences are small. The sparse data seems to indicate that there is no prominent decrease around the official TLE epoch, either.

4 Orbit Determination and Propagation with CelMech

4.1 Selected Objects, Data Density and Spacing

To investigate the orbit determination and propagation process routinely performed for the internal catalogue of the AIUB in more detail, four representative objects from the internal catalogue of the AIUB were chosen, which are not in the USSTRATCOM catalogue and have been followed over longer time periods. Those objects are clearly space debris, since no maneuvers could be detected in the data. The AIUB did not have information what those objects actually were before becoming debris. From the apparent magnitude it can be concluded that those are all fragmentation pieces. Therefore, they represent typical objects found in GEO surveys. Their properties are listed in Tab. 1.

The available optical measurements are plotted in Fig. 4 through 6. The observations are binned for each night. The Zimmerwald observations were obtained from ZIMLAT and ZimSMART, the Tenerife observations from ESASDT, and the supplementary observations from ISON, which come from from different sensors in Eastern Europe.

Table 1: Internal name, eccentricity, inclination (deg), semi-major axis (km), area to mass ratio (m^2/kg) and apparent magnitude (mag) of the selected objects of the AIUB catalogue

NAME	E	I	A	A/M	Mag
E03174A	0.001	10.1	41900	0.01	14.6
E06321D	0.036	7.0	42900	2.46	15.3
E06327E	0.060	11.9	42400	0.326	17.2
E08241A	0.040	13.26	43200	1.20	16.1

4.2 Residuals from Single and Combined Sites

With the available data, orbit determinations and propagation were performed with an enhanced version of the CelMech tool. The propagated ephemerides were correlated with the COROBS tool using additional observations which were not used in the orbit determination process. All observations were obtained from ZIMLAT and ESASDT, and all data was cross-checked via independent orbit determinations. There were no observations from ISON used as reference data.

Different orbits were determined for the ZIMLAT data and the ESASDT data separately. In the second step, data of both sites were combined; if data was available, supplementary ISON data was used in the combined step, too. To get comparable results, a maximum of six observations at the beginning of the observational fit arc was used for orbit determination and a maximum eight observations at the end of the fit span. At minimum, there were three observations used at each end. The observations itself can consist of more than one tracklet. When observations from different sites are used, either the first set of observations stem from one site and the second from another or there are observations from different sites at similar epochs used within the first and/or the last set of observations or a mixture of those options. No additional observations in between were used.

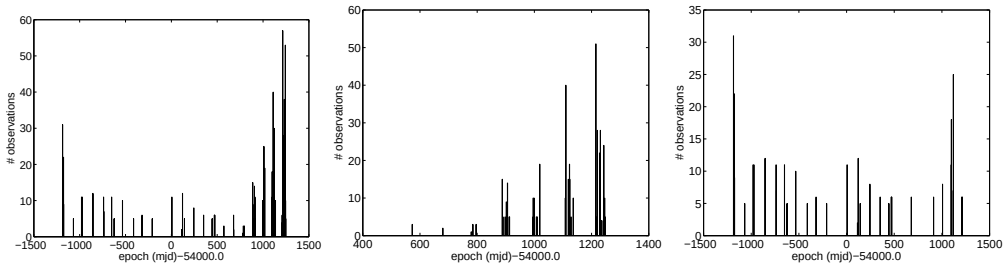

(a) *(b)* *(c)*

Figure 3: Data density of object E03174A (a) all observations, (b) Zimmerwald, (c) Tenerife

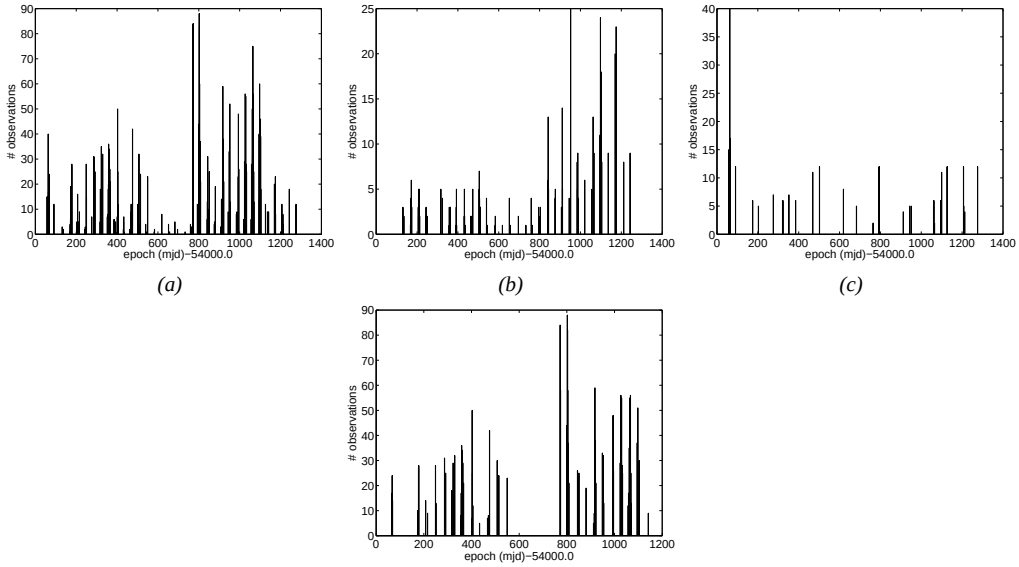

(a) *(b)* *(c)*

(d)

Figure 4: Data density of object E06321D (a) all observations, (b) Zimmerwald, (c) Tenerife, (d) ISON network

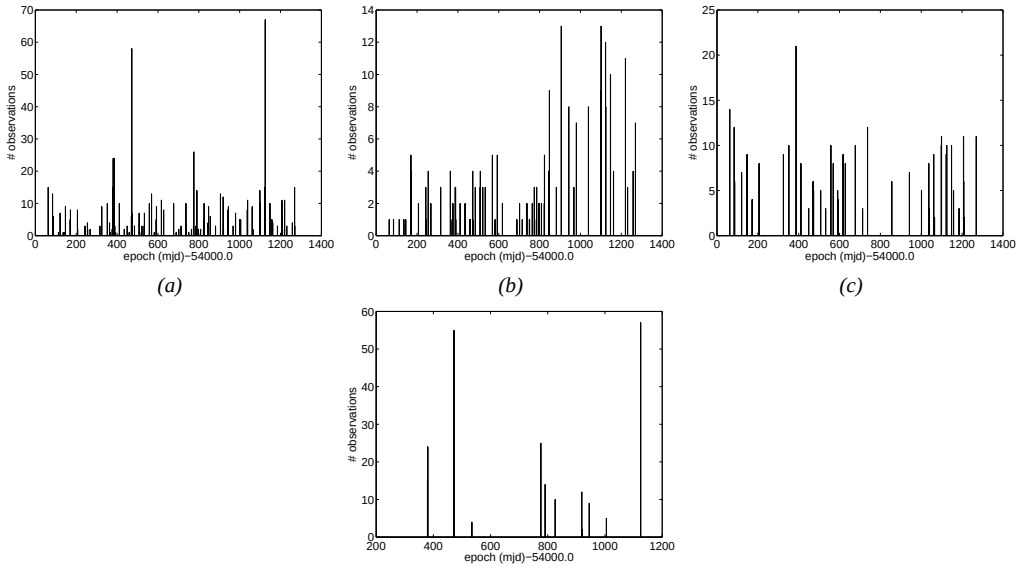

(a) *(b)* *(c)*

(d)

Figure 5: Data density of object E06327E (a) all observations, (b) Zimmerwald, (c) Tenerife, (d) ISON network

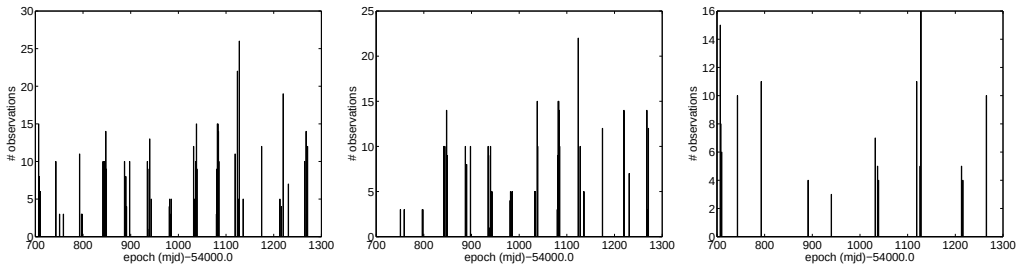

(a) *(b)* *(c)*

Figure 6: Data density of object E08241A, (a) all observations, (b) Zimmerwald, (c) Tenerife

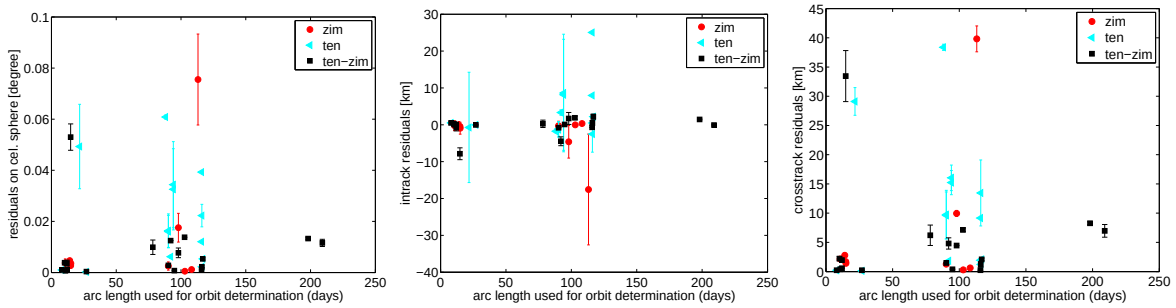

(a) *(b)* *(c)*

Figure 7: Mean value and standard deviation of residuals within the first 50 days after orbit determination between propagated and observed positions of object E03174A as a function of the arc length between the first and last observations used for orbit determination: (a) position residual on celestial sphere (degree), (b) projected intrack residuals, (c) projected crosstrack residuals

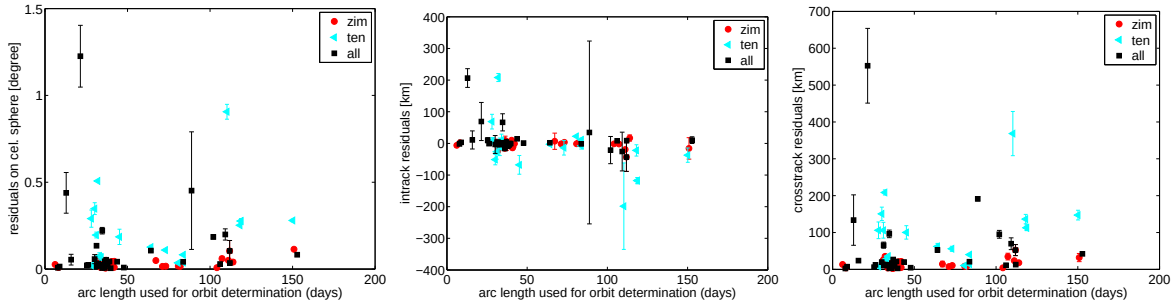

(a) *(b)* *(c)*

Figure 8: Mean value and standard deviation of residuals within the first 50 days after orbit determination between propagated and observed positions of object E06321D as a function of the arc length between the first and last observations used for orbit determination: (a) position residual on celestial sphere (degree), (b) projected intrack residuals, (c) projected crosstrack residuals

In Fig. 7 through Fig. 10 the residuals between predicted and observed position are displayed in arc length on the celestial sphere, and in projected intrack and crosstrack direction as a function of the arc length between the first and the second set of observations, which were used in orbit determination. Displayed are the mean values and the standard deviations of residuals of the single orbits. The mean value and standard deviations are determined out of single residuals of predicted position to observed ones, all within 50 days since orbit determination. For the mean values and standard deviations, six to 30 single residuals were used.

What can be seen in Fig. 7 through Fig. 10 is that the residuals are in general – even though only a small amount of data was used – are all very small. The vast majority of the detemined orbits even produce residuals smaller than 0.6 degree. Except for the first object, each object also shows some outliers, with larger residuals. These larger residuals also tend to show larger standard deviations. It can also be seen, that the larger residuals not only show up in the projected intrack direction but also in crosstrack direction – it is not just a runaway argument of an ill-defined semi-major axis. In addition, the value of the residuals seems to be, at least in this setup, quite independent of how large the difference between the first and the second observations set is. Moreover, Fig. 7 through Fig. 10 also show that there is no significant difference in using observations only from one observation site for orbit determination or using observations from different sites. It could not be shown that the latter approach is more advantagous for orbit determination. Different observation sites still have advantages in terms of availability, weather conditions, and so on. In Fig. 11, the root mean square of the orbit determinations is shown, which were used for the propagation, as a function of the arc residuals. It shows that no trend is visible, all orbits which were used had a small root mean square of below three arcseconds. From the orbit determination alone it cannot be uniquely concluded how good the propagation will be. For the orbit determination with CelMech biases can be estimated, but are not available for orbit determination. Fig. 12 shows the arc length residuals on the celestial sphere as a function of the number of estimated parameters in addition to the osculating elements. If only one parameter is estimated, only the advanced model for direct radiation pressure and a new area-to-mass value was estimated. If two or three parameters are estimated, in addition to the DRP either only the R-bias or the R- and the W-bias (RSW coordinate system) were estimated. Although the biases cannot be used for the propagation, it cannot automatically be concluded that the propagated orbit produces large residuals.
In Fig. 13, the area-to-mass ratio, which was determined from the estimated direct radiation pressure, is displayed. It can be observed,

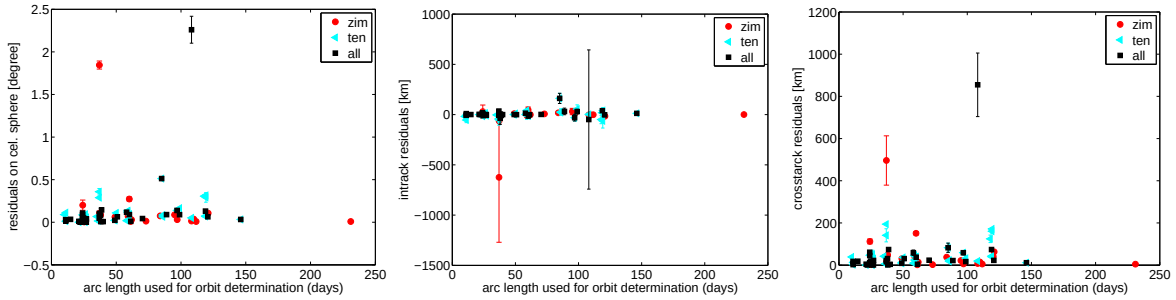

(a) *(b)* *(c)*

Figure 9: Mean value and standard deviation of residuals within the first 50 days after orbit determination between propagated and observed positions of object E06327E as a function of the arc length between the first and last observations used for orbit determination: (a) position residual on celestial sphere (degree), (b) projected intrack residuals, (c) projected crosstrack residuals

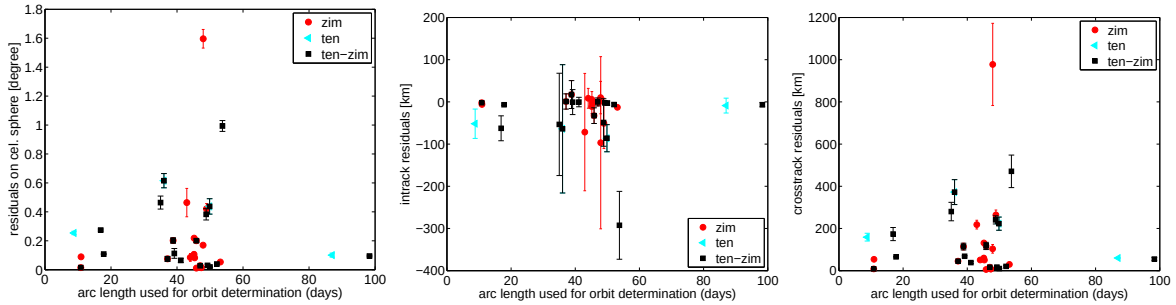

(a) *(b)* *(c)*

Figure 10: Mean value and standard deviation of residuals within the first 50 days after orbit determination between propagated and observed positions of object E08241A as a function of the arc length between the first and last observations used for orbit determination: (a) position residual on celestial sphere (degree), (b) projected intrack residuals, (c) projected crosstrack residuals

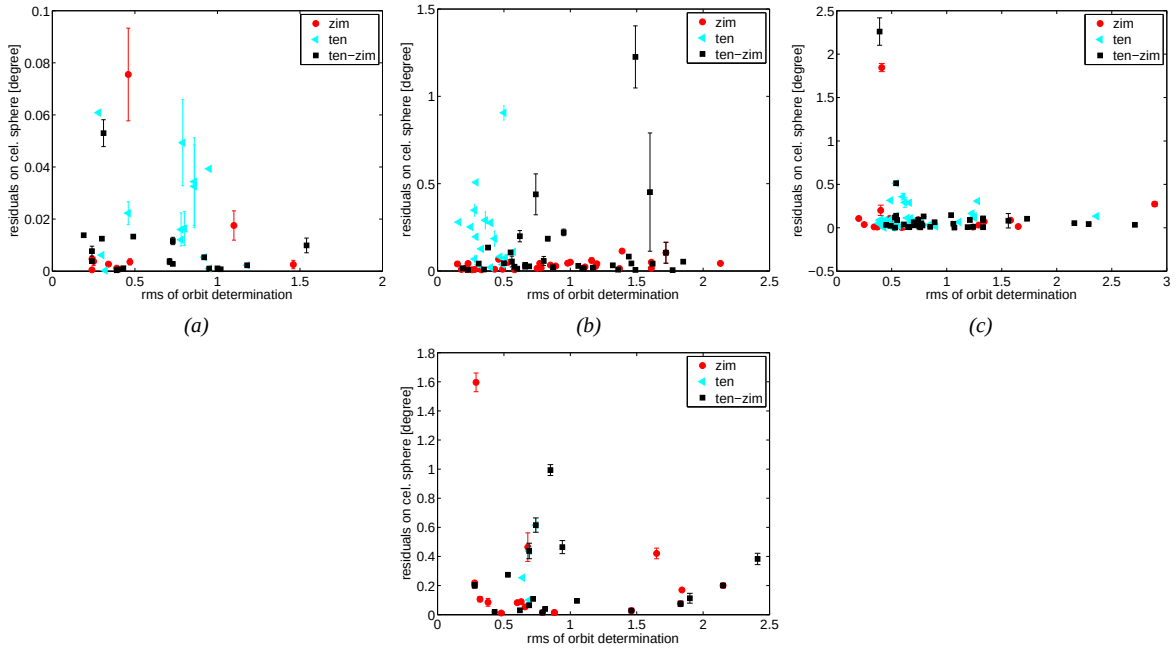

(a) *(b)* *(c)*

(d)

Figure 11: Root mean square of orbit determination as a function of the arc elngth of observations.

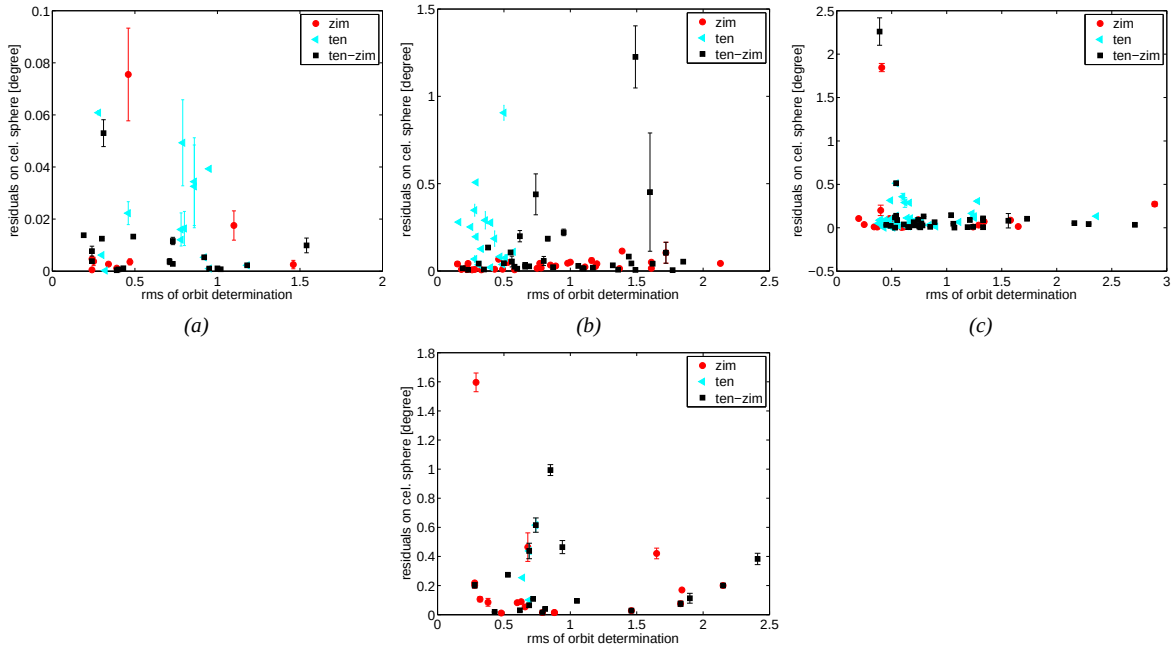

Figure 12: Arc length residuals as a function of the number of additional solve-for parameters, that were estimated: (1) DRP (2) DRP and R-bias, (3) DRP, R-bias, and W-bias (RSW coordinate system)

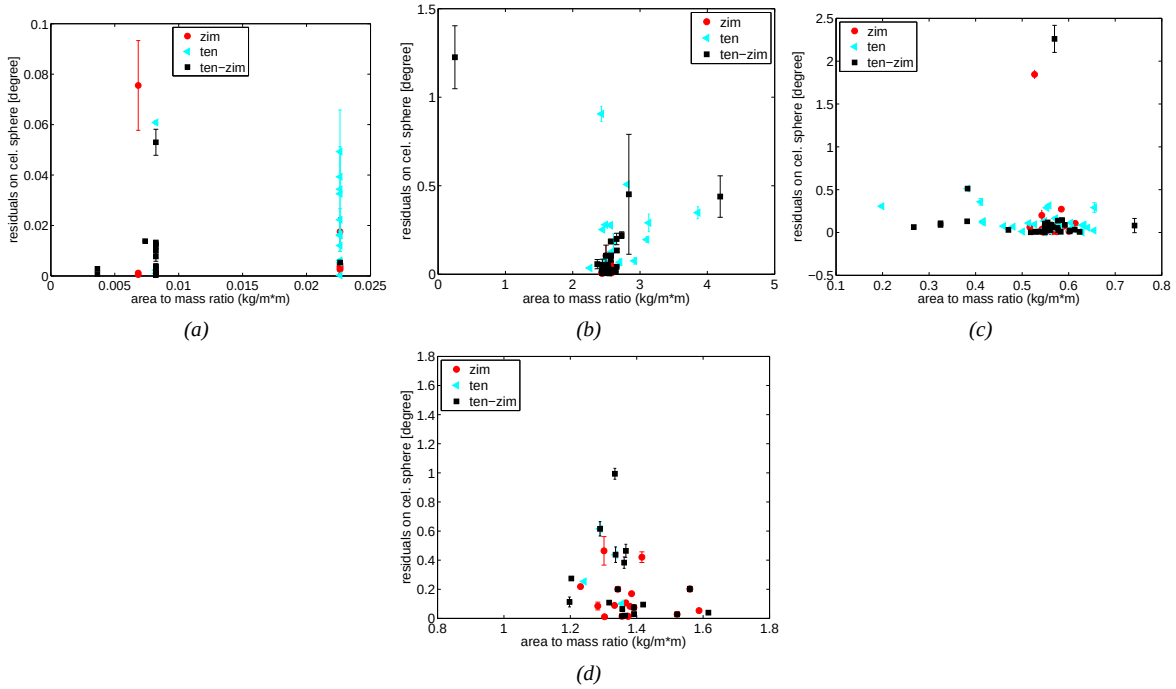

Figure 13: arc length on the celestial sphere as a function of the estimated area-to-mass ratio.

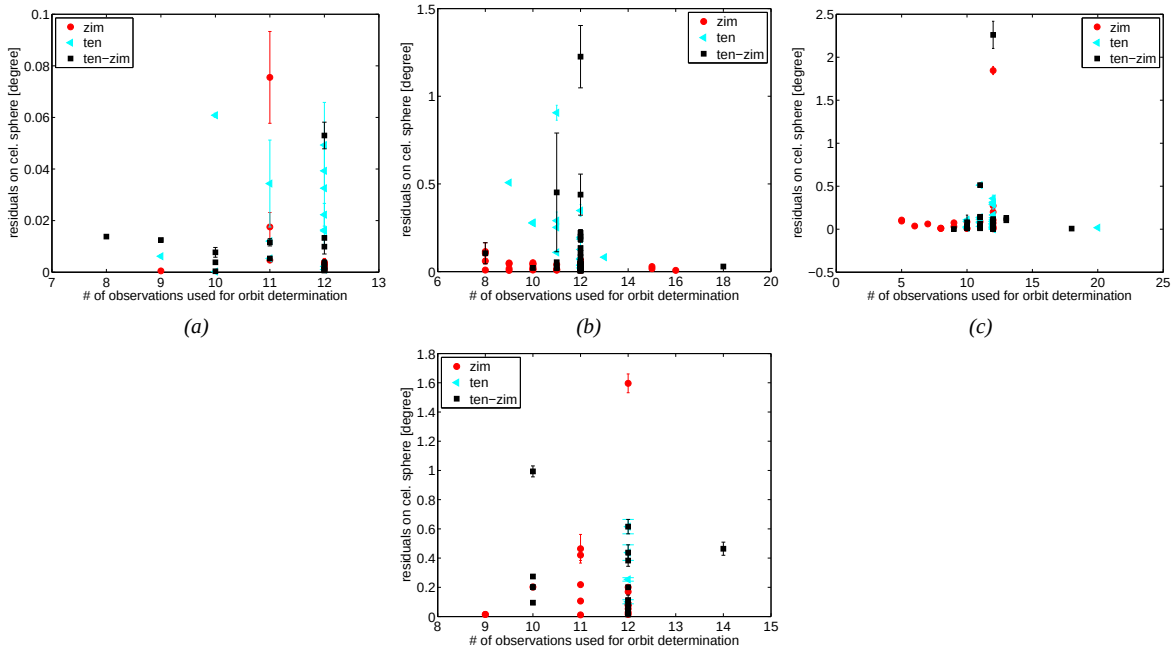

Figure 14: Arc length residuals as a function of the number of observations used for orbit determination

that the area-to-mass ratios of the different objects vary over different ranges. It can also be seen that in some orbit determinations values were determined, which are far off the median area-to-mass ratio value for that specific object. These, in most cases, also lead to large residuals in the propagated orbits. This suggests that there seem to be short periodic changes in the area-to-mass ratio.

In Fig. 14, the arc length residuals on the celestial sphere are displayed as a function of the actual number of single observations that entered orbit determination. It can be seen that no strong correlation is visible between the actual number of observations used and the value for the residuals. More importantly, seems to be the arc length of the observations itself. In Fig 15, the arc length residuals are displayed as a function of the actual arc length within the two sets used in the beginning and the end of the fit arc, without the time gap in between the two sets. A strong correlation is visible. Fig. 16 shows that there is no strong correlation between the number of used observations and the arc length within the sets. For example,for the Tenerife observation strategy, primarily densely spaced observations are available.

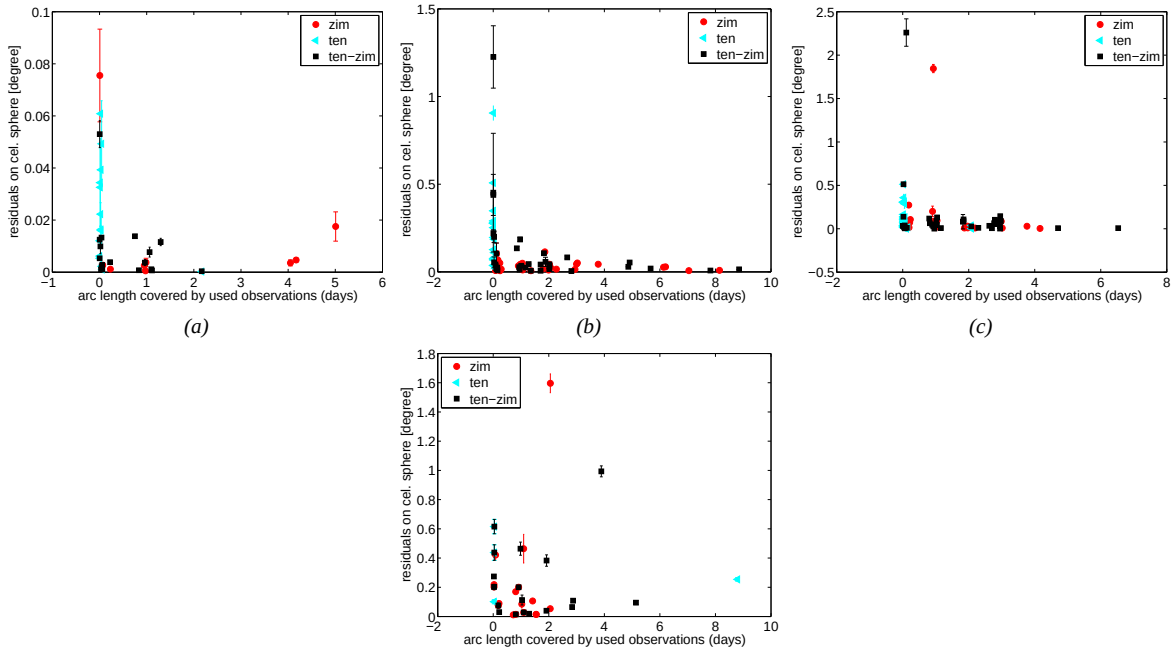

Figure 15: Residuals in arc length on the celestrical sphere as a function of arc length covered by observations used for orbit determination.

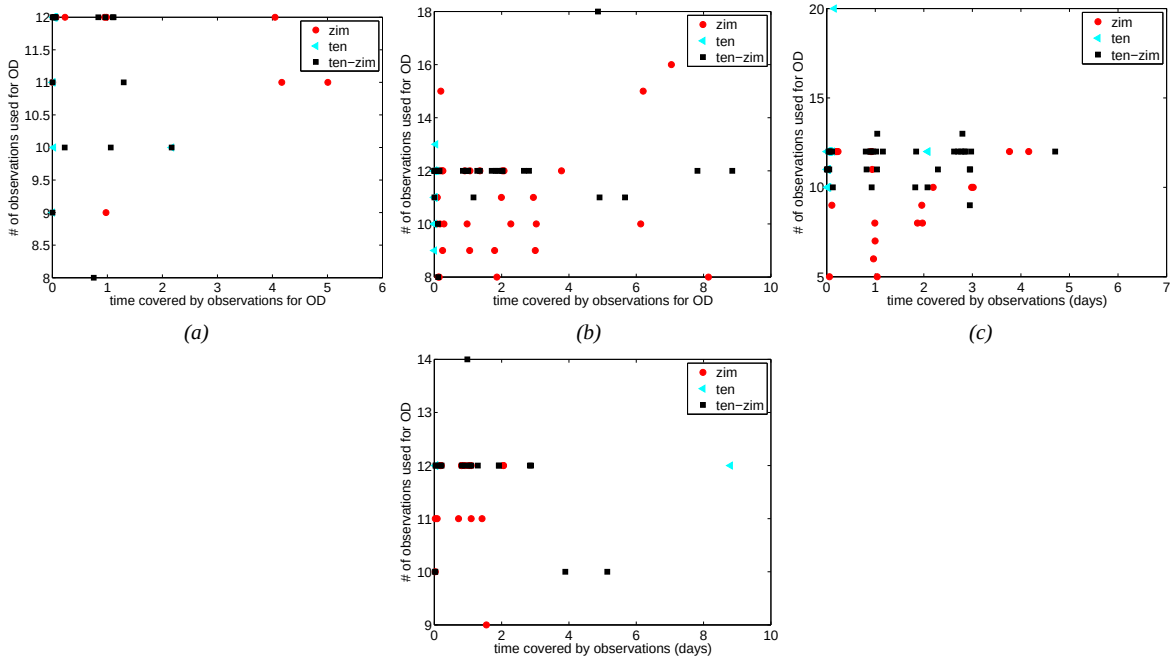

Figure 16: Arc length covered by the observations as a function of the number of observations used for orbit determination.

5 Conclusions

In this paper, examples of the accuracy of orbit propagation were investigated for orbits using TLE data from USSTRATCOM and orbits from the AIUB catalogue determined with the CelMech tool under controlled conditions.

In case of the TLE data, propagation was performed with the SDP4 and SDP8 propagators. In case of the AIUB orbits, with the CelMech tool. The ephemerides of the propagated orbits were compared, using the COROBS tool, with optical angle-only observations as ground truth.

The examples of the TLE data used in the investigation seems to suggest that the effect of the different propagators is negligible for objects in geostationary orbits. Slightly better results are achieved for the SDP4 propagator for objects in highly eccentric orbits compared to the SDP8 propagator.

Regarding the accuracy of orbit determination and propagation of orbits in the internal AIUB catalogue, the influence of sparse data sampling of angle-only observations from different observation sites for different lengths of observations arcs used in orbit determination was investigated in a controlled setup of only two data sets at the beginning and the end of the fit arc.

The vast majority showed residuals of below 0.6 degrees within 50 days after orbit determination, even with such a sparse data sampling; even the largest residuals were found to be below 2.5 degrees. No strong correlation was found for the value of the residuals to the time gap between the two data sets used. A strong dependence on the use of observations of one or more observation sites could not be observed. The actual number of observations used in this specific setup was less critical than the arc length within each of the two observation sets used for orbit determination. This seems to suggest that precise orbit determination, which allows finding an object again in follow-up observations, is possible even for sparse data sampling – which could be due to bad weather conditions, system failures and so on – as long as a mimimum arc is covered by the actual observations used.

6 ACKNOWLEDGMENTS

Special thank goes to ISON and the Keldish Institute of Applied Mathematics, Moscow for the supplementary observations.
The work was supported by the Swiss National Science Foundation through grants 200020-109527 and 200020-122070.

The observations from the ESASDT were acquired under ESA/ESOC contracts 15836/01/D/HK and 17835/03/D/HK.

REFERENCES

[1] R. Musci, T. Schildknecht, M. Ploner, and G. Beutler. Orbit Improvement for GTO Objects Using Follow-up Obervations. *Advances in Space Research*, 35(7):1236–1242, 2005.

[2] D. Vallado and S. Carter. Accurate Orbit Determination from Short-arc Dense Observational Data . In *Proceedings of the AAS/AIAA Astrodynamics Specialist Conference,Sun Vallex, ID, AAS 97-704*, 1997.

[3] G. Beutler. *Methods of Celestial Mechanics*. two volumes. Springer-Verlag, Heidelberg, 2005. ISBN: 3-540-40749-9 and 3-540-40750-1.

[4] F.R. Hoots and R.L. Roehrich. Models for Propagation of NORAD Element Sets. *Spacetrack Report*, No. 3, 1980.

[5] C. Früh, T. Schildknecht, R. Musci, and M. Ploner. Catalogue Correlation of Space Debris Objects. In *Proceedings of the Fifth European Conference on Space Debris, ESOC, Darmstadt, Germany, 30 March-2 April 2009*, 2009.

[6] C. Früh, T. Schildknecht, and M. Ploner. Comparison of different Methods of Ephemeris Retrival for Correlation of Observations of Space Debris Objects. In *Proceedings of the 2009 AMOS Technical Conference, 1-4 September 2009, Maui, Hawaii, USA*, 2009.

[7] T.S. Kelso. Validation of SGP4 and IS-GPS-200D Against GPS Precision Ephemeris . In *Proceedings of the 17th AAS/AIAA Space Flight Mechanics Conference, Arizona, Jan 28th - Feb 1st, 2007, AAS 07-127*, volume Sedona, Arizona, 2007.

7 Appendix:

Table 2: GEO objects: COSPAR number and epoch as displayed in the TLEs.

COSPAR	epoch
02040B	9073.16
78035A	5029.65
79105A	5298.79
80081A	6072.67
82044F	6303.96
83089B	6303.96
84035A	7359.67
85035B	8324.71
90061D	8324.79
91010F	8289.16
92088A	8289.06
93073B	7070.85
97049B	9015.72
99047E	8202.46

Table 3: HEO objects: COSPAR number and epoch as displayed in the TLEs.

COSPAR	epoch
00016C	8247.25
00067D	9014.34
00068B	9053.41
70055B	8036.02
77105A	8290.06
88018C	9020.14
91015P	9021.19
91084C	8052.04